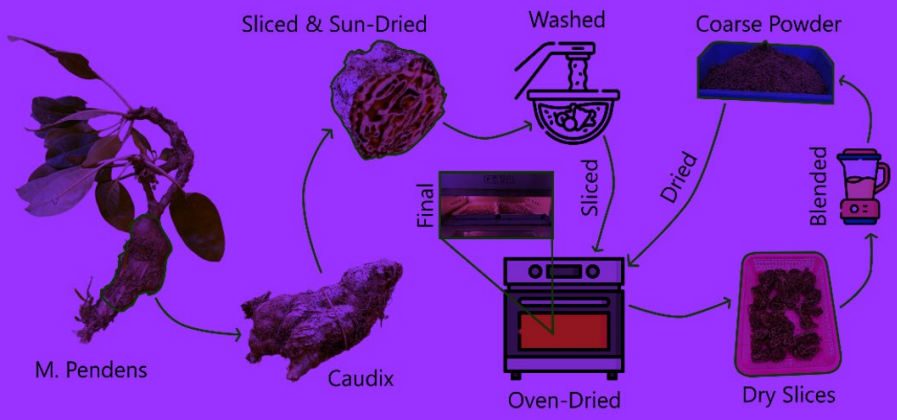

BJP

Bangladesh Journal of Pharmacology

Research Article

Diabetic wound healing activity of *Myrmecodia pendens* ethyl acetate fraction

A Journal of the Bangladesh Pharmacological Society (BDPS)
Journal homepage: www.bdpsjournal.org; www.banglajol.info
Abstracted/indexed in Academic Search Complete, Agroforestry Abstracts, Asia Journals Online, Bangladesh Journals Online, Biological Abstracts, BIOSIS Previews, CAB Abstracts, Current Abstracts, Directory of Open Access Journals, EMBASE/Excerpta Medica, Global Health, Google Scholar, HINARI (WHO), International Pharmaceutical Abstracts, Open J-gate, Science Citation Index Expanded, SCOPUS and Social Sciences Citation Index
ISSN: 1991-0088

Bangladesh J Pharmacol 2025; 20: 62-71

Diabetic wound healing activity of *Myrmecodia pendens* ethyl acetate fraction

Yuniarti Falya[1], Abd Kakhar Umar[2], Ine Suharyani[3], and Cindra Yulianto Anugra[3]

[1]Faculty of Pharmacy, Universitas Islam Kalimantan Muhammad Arsyad Al Banjari, Banjarmasin, South Borneo, Indonesia; [2]Medical Informatics Laboratory, ETFLIN, Palu City 94225, Indonesia; [3]Faculty of Pharmacy, Universitas Muhammadiyah Ahmad Dahlan Cirebon, Cirebon 45153, Indonesia.

Article Info

Received: 6 March 2025
Accepted: 21 May 2025
Available Online: 23 May 2025
DOI: 10.3329/bjp.v20i2.80330

Cite this article:
Falya Y, Umar AK, Suharyani I, Anugra CY. Diabetic wound healing activity of *Myrmecodia pendens* ethyl acetate fraction. Bangladesh J Pharmacol. 2025; 20: 62-71.

Abstract

This study investigates the diabetic wound healing potential of *M. pendens* using an *in vivo* diabetic animal model and molecular docking targeting MMP, EGF, and FGF pathways. Ethyl acetate hydrogel formulations (0.05%, 0.10%, and 0.15%) were tested over 14 days, with wound closure measured using ImageJ. The fraction contained 91.5 mg QE/g of flavonoids. Docking analysis showed strong binding affinities of quercetin, cholesta-22,24-dien-5-ol, and procyanidin B1 to MMP, EGFR, and FGFR (−8.4 to −10.2 kcal/mol). By day 14, the negative control group showed 30-40% wound closure, while tetrachlorodecaoxide reached 80% ($p<0.01$). The 0.05% hydrogel achieved 85% closure ($p<0.05$), and the 0.10% hydrogel showed complete healing (100%, $p<0.001$). The 0.15% hydrogel was less effective than 0.10%, with significant differences between days 7 and 14 ($p<0.05$). These findings suggest that *M. pendens* hydrogel may aid diabetic wound healing through molecular pathway modulation.

Introduction

Diabetic wound is among the most serious complications of diabetes, with high morbidity rates. Although approximately 60–80% of the diabetic wound can heal, 10–15% remain chronic, and 5–24% of cases result in amputation within 6 to 18 months (McDermott et al., 2023). Neuropathic ulcer often requires more than 20 weeks to heal, while neuroischemic wound takes even longer and carry a higher risk of amputation (Boulton and Whitehouse, 2000; Alexiadou and Doupis, 2012). Beyond being a significant health burden, diabetic wound also imposes substantial financial pressure due to prolonged medical care, advanced wound therapies, and surgical intervention such as amputation in severe case. Unlike normal wound healing, diabetic wound takes longer time to heal (Spampinato et al., 2020; Burgess et al., 2021). This is due to its inability to progress to the proliferative phase and the persistence of chronic inflammation. This wound is characterized by unique conditions such as high moisture level, elevated blood sugar, hypercoagulability, and weakened immune response. These factors increase the risk of infection, hinder nutrient supply to the wound tissue, and slow the healing process (Dasari et al., 2021).

Therefore, managing diabetic wound requires a complex therapeutic approach.

One promising solution is to use multiple compounds present in natural products, which work synergistically to support the wound healing process. Natural products that exhibit anti-inflammatory activity, suppress or inhibit microbial growth, and modulate cytokines and growth factors are potential therapeutic leads for

treating diabetic wound.

There are several plants that have potential diabetic wound healing activity, including *Crocus sativus* (saffron) (Soheilifar et al., 2024); *Musa paradisiaca* (Cheng et al., 2020); *Sphenocentrum jollyanum* pierre (Adeleke et al., 2022)., and *Myrmecodia pendens* (Najah et al., 2024).

Myrmecodia pendens has antioxidant, antimicrobial, and immunomodulatory properties (Sudiono et al., 2015; Widyawati et al., 2020; Dirgantara et al., 2022; Daulay et al., 2024; Lisnanti et al., 2024). Its diabetic wound-healing effect has not yet been examined. In addition, this study aimed to explore its ability to modulate key molecular pathways such as matrix metalloproteinases (MMP), epidermal growth factor receptor (EGFR), and fibroblast growth factor receptor (FGFR), supported by phytochemical, *in silico*, and *in vivo* evaluations.

The ethyl acetate fraction of *M pendens* extract is known to contain flavonoids that have been shown to positively regulate MMP-2, MMP-8, MMP-9, MMP-13, and the Ras/Raf/MEK/ERK, PI3K/Akt, and nitric oxide (NO) signaling pathways (Chanu et al., 2023). Compounds such as procyanidin B1 dimer (3.2 mg/g dry sample) and rosmarinic acid (20.7 mg/g dry sample) exhibit significant free radical scavenging activity, with IC_{50} values of 27.6 µg/mL and 35.8 µg/mL, respectively (Engida et al., 2015). Additionally, six phenolic and terpenoid compounds have been identified in *M. pendens*, some of which show antibacterial activity against various pathogenic bacteria, including dibenzo-p-dioxin-2,8-dicarboxylic acid exhibits an inhibition zone of 8.6 mm against *E. faecalis*, while stigmast-4-ene-3-one and pomolic acid show inhibition zones of 9.0 mm and 10.2 mm against *S. mutans*, respectively. Phloroglucinol sesquiterpene demonstrates the largest inhibition zone of 12.3 mm against *P. gingivalis*. Other studies have reported that the ethyl acetate fraction of *M. pendens* exhibits antibacterial activity against *S. mutans* biofilms at a concentration of 50 µg/mL, with a Minimum Biofilm Eradication Concentration (MBEC) of 40% for a one-minute induction period (Gartika et al., 2018). A combination of hexane-ethyl acetate fractions shows the best antibacterial activity, with a Minimum Inhibitory Concentration (MIC) of 0.05 mg/mL and a Minimum Bactericidal Concentration (MBC) of 12.5 mg/mL (Kuswandani et al., 2019). This study explores the potential of ethyl acetate fraction-based hydrogel of *M pendens* for diabetic wound healing, both *in silico* and *in vivo*.

Materials and Methods

The materials used include *M pendens* plants sourced from Borneo, West Kalimantan, filter paper (Whatman® Grade 1), aquadest (Brataco®), 70% ethanol (Sigma-Aldrich®), n-hexane (Merck®), chloroform (Merck®), sodium hydroxide (Sigma-Aldrich®), 0.1% ferric chloride/FeCl3 (Merck®), sulfuric acid (Sigma-Aldrich®), hydrochloric acid (Merck®), aluminum chloride (Sigma-Aldrich®), methanol (Merck®), Dragendorff's, Carbopol (Carbopol 940), hydroxypropyl methylcellulose/HPMC (Ashland® Benecel™), glycerin (Brataco®), methylparaben (Brataco®), propylparaben (Brataco®), triethanolamine (Merck®), and phosphate-buffered saline.

Plant collection, identification, and simplification

This plant is an epiphytic species that grows attached to various types of trees. When collected, the plants were harvested randomly from several tree species that were not identified at the time. The plants were sourced from the Nanga Pinoh region of West Kalimantan, Indonesia, and subsequently identified as *M. pendens* by Prof. Ria Yulia Gloria, at Biology Laboratory of the State Islamic Institute of Syekh Nurjati Cirebon, with notification number 30/LN.08/LB.1.1/PP.009/12/2023. The part of the plant collected was the caudex (the swollen, hollow stem), which was separated and brought to the pharmacognosy laboratory for further processing.

The outer surface of the caudex was initially cleaned of dirt and fibrous roots. It was then split and cut into large sections, which were sun-dried to remove ants. Once all sections were free from ants, they were sliced into thin, flat pieces approximately 1 cm thick and washed to remove soil, debris, and ant eggs. Sections with inconsistent tissue characteristics (e.g., at the junctions of the caudex with the stem or roots) were discarded. The cleaned slices were then oven-dried at 40°C for one week. The dried pieces were subsequently referred to and labeled as simplicia.

Extraction and fractionation

The dried simplicia was blended until it became a coarse powder and dried in an oven for a day (40°C). The coarse powder (350 g) was then moistened with 70% ethanol until all parts were submerged. This maceration process was carried out for 3 days at room temperature (25°C) with regular manual shaking (twice a day). The solution was then filtered to obtain a dilute extract solution. The residue was, then, remacerated following the same procedure as before. This process was repeated three times. The filtrates from these processes were combined, and the solvent was then evaporated using a rotary evaporator at 40°C, 200 mBar, and 150 rpm until a thick extract consistency was achieved.

The extract was subsequently fractionated using ethyl acetate and water in a 1:1 ratio. The two phases were then separated, and the ethyl acetate phase was further dried using a rotary evaporator until a thick fraction was obtained.

Simplician and extract standardization

M. pendens simplicia was standardized to ensure its quality and consistency by assessing key parameters as described in the Indonesian Herbal Pharmacopoeia. The analyzed parameters included organoleptic properties, water-soluble content, ethanol-soluble content, moisture content, total ash content, acid-insoluble ash content, and percentage of drying loss.

Phytochemical screening

The crude methanolic extract and fractions of *M pendens* were analyzed for phytochemical constituents, including alkaloids, flavonoids, steroids, tannins, saponins, terpenoids, and phenolics. Phytochemical reagents were added to the extract and fraction solutions, and the qualitative results were recorded as the presence and the absence of each phytochemical**.**

Total flavonoid content

Total flavonoid content of the ethyl acetate extract was determined using the aluminum chloride colorimetric method and using standard solutions (4, 5, 6, 7, and 9 ppm). For the analysis, 1 mL extract solution in 80% methanol (1 mg/mL) was mixed with 0.5 mL 95% ethanol (v/v), 0.2 mL aluminum chloride solution (10%), 0.2 mL 1 M potassium acetate, and 1 mL distilled water to a total volume of 2.5 mL. The mixture was well mixed and incubated at room temperature for 30 min. Total flavonoids were measured using a UV-Vis spectrophotometer at wavelengths 520 nm vs. a reagent blank containing water instead of the sample. Quercetin was used as the standard for the quantification of total flavonoids. Results were expressed as milligrams of quercetin equivalent per gram of dry weight extract (mg QE/g). Total content of flavonoid was calculated as follows:

Total flavonoid content = QE × V/m

Where QE is the quercetin equivalence (mg/mL) or concentration of quercetin solution established from the calibration curve; V is the volume of extract (mL), and m is the weight (g) of the dry extract (Sulastri et al., 2018)

FTIR analysis

Approximately 2 mg of each sample fraction was weighed and thoroughly mixed with 100 mg of dry potassium bromide powder. The mixture is then homogenized to ensure an even distribution of the sample in the potassium bromide and pressed into a thin, transparent disc using a high-pressure hydraulic press (approximately 10 tons of pressure). The potassium bromide disc was then placed in the FT-IR spectrometer, where scanning was performed in the infrared range of 4000–400 cm^{-1}. Before analyzing the sample, a background spectrum (air) was recorded to eliminate atmospheric interference (Ol'ha and Hovorun, 2021).

Computational study

Ligand preparation

A total of 70 compounds from 3 literature sources were collected (6-8), and structures with the same CID were manually removed. The 2D structures were then converted to 3D using Open Babel in PDB format. Similar structures and molecules with identical descriptors were also removed using the --unique command in Open Babel. The structures were protonated at pH 7.4, and charges were added using the MMFF94 force field. Before saving, the energy of the compounds was minimized, and the MMFF94 force field was applied. All PDB files were converted to PDBQT format using the repair_ligand4.py script. The entire process was performed simultaneously using custom Python code.

Receptor preparation

The structures of EGFR, FGFR, and MMP were obtained from the RCSB with IDs MMP [1CIZ], EGFR [2GS6], FGFR [4QQ5]. Water molecules, ions, and non-ligand compounds were removed using Discovery Studio. The position of the native ligand was set as grid coordinates, with the grid size adjusted to match the native ligand's structure. The native ligand was then separated and saved as a PDB file. The native ligand was prepared following the same process as the test ligands until it was in PDBQT format. The cleaned protein structure was saved as a PDB file. The protein structure was subsequently input into AutoDock Tools, where Kollman charges were applied, polar hydrogens were added, and the structure was saved in PDBQT format. Finally, the initial native ligand structure and the pose after docking were superimposed, and the RMSD value was calculated as a validation of the docking method.

Molecular docking

Molecular docking was performed using DockFlin (Version 2.0, ETFLIN, Indonesia). All ligands and proteins were loaded into their respective panels. The grid files, containing the coordinates and size, were input according to the sequence of the proteins in the panel. After setting the output folder, the docking process was initiated using the Vina scoring function.

Diabetic wound activity

Animal preparation

Forty male Wistar rats (aged 8-10 weeks, weighing 180-220 g) were used in the study and were adapted to cage conditions for two weeks. Subsequently, the rats were given a special diabetes diet (diabetic rat feed) for another two weeks. Before the diet, the rats were induced with alloxan 110 mg/kg via intraperitoneal injection. At the end of the diet period, which lasted for 7 days post-alloxan induction, fasting blood glucose levels were measured to confirm diabetes, blood

glucose levels of the rats were measured using a digital glucometer (Autocheck®), and those with hyperglycemia (140-220 mg/dL) were included in the study.

Wound creation and treatment

Wound creation began with shaving the dorsal fur using an electric shaver, followed by anesthesia with ketamine administered intraperitoneally at the wound site. A full-thickness wound was induced using a 4 mm biopsy punch, and the initial wound size was recorded using a camera positioned 30 cm away from the wound. Daily treatment was administered for 14 days, with wound size assessed on day 0, 3, 5, 7, 9, and 14. The rats were divided into five treatment groups (6 rats per group): a negative control group (hydrogel base), a positive control group (tetrachlorodecaoxide hydrogel), and three experimental groups treated with varying concentrations of the ethyl acetate fraction of *M pendens* (0.05%, 0.10%, and 0.15%) in a hydrogel base. The hydrogel base was prepared by dissolving 0.5% hydroxypropyl methylcellulose in water. Wound healing was assessed by calculating the percentage of wound coverage, determined by comparing the initial wound area with the area at each observation point.

Statistical analysis

Statistical analysis was performed to determine the significance of differences between the treatment groups in the *in vivo* study. One-way ANOVA followed by post hoc testing using the Tukey method was applied using RStudio (version 2024.09.1).

Results

Extract standardization and phytochemicals

M. pendens ethyl acetate extract contained various bioactive compound groups, including alkaloids, flavonoids, terpenoids, tannins, and saponins (data not shown). The total flavonoid content in the *M. pendens* extract was found as 48.5 mg QE/g (4.9 ± 0.9% QE), while in the ethyl acetate, the value significantly increased to 91.5 mg QE/g (91.5 ± 0.014% QE).

The peaks at 3341 cm^{-1} and 1564 cm^{-1} show a significant absorbance, indicating that the ethyl acetate fraction of *M pendens* contained compounds with numerous hydroxyl or phenolic groups (carboxyl or phenolic; Figure 1). This is further supported by 937 cm^{-1} and 503 cm^{-1} peaks, which are characteristic signs of C-O coupled with O-H and cis-HCOOH.

Extract hydrogel formulation

Figure 2 presents the organoleptic analysis results of four hydrogel formulas. In terms of aroma, all formulas exhibited a stable characteristic scent throughout the storage period. However, the formulas containing the ethyl acetate fraction of *M pendens* (0.05%, 0.10%, and 0.15%) showed a slight increase in aroma intensity compared to the base formula A (Figure 2A). Regarding color, each formula displayed distinct differences. The base formula was white, while formulas containing the ethyl acetate fraction of *M. pendens* showed a gradient of yellow, deepening as the extract concentration increased. The 0.05% formula had a clear yellow color, the 0.10% formula was dark yellow, and the 0.15% formula appeared yellow-brown.

In terms of texture, all hydrogel formulas exhibited a smooth consistency and were easy to apply to the skin. The base formula, without any extract, had a light, non-sticky texture and provided a soft sensation upon application, which can be attributed to hydroxypropyl methylcellulose gel that was lightweight and non-sticky. In contrast, the formulas containing the ethyl acetate fraction of *M. pendens* (0.05%, 0.10%, and 0.15%) showed a thicker and slightly stickier texture, with

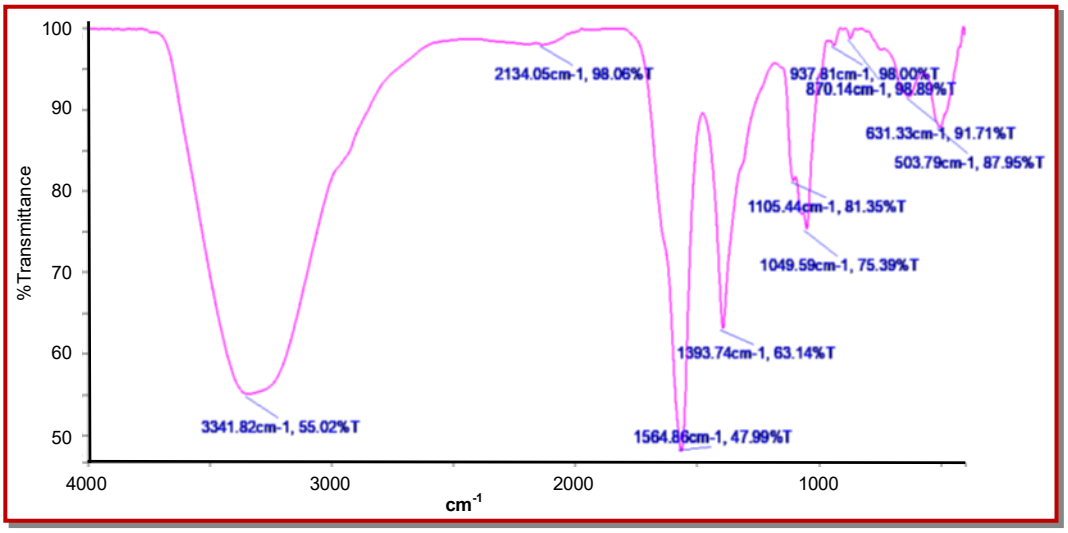

Figure 1: FT-IR spectrum ethyl acetate fraction of *M. pendens*

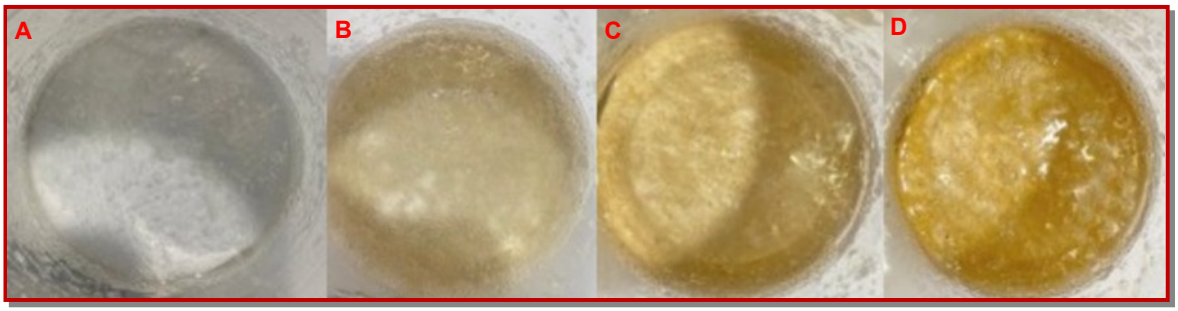

Figure 2: Hydrogel formulations - base (A); formula 0.05% (B); formula 0.10% (C); formula 0.15% (D)

viscosity increasing as the extract concentration rose.

Molecular docking

Method validation was carried out through the redocking process of the native ligand into the binding site of each receptor to calculate the Root Mean Square Deviation (RMSD) value and evaluate the accuracy of the method used. The redocking results shown in Figure 3 A-C indicate RMSD values of 0.0251 Å for MMP, 1.6272 Å for EGFR, and 1.1429 Å for FGFR. The low RMSD values (≤2.0 Å) for all three complexes suggest that the docking method successfully replicated the position and orientation of the native ligand within the binding site with a high degree of accuracy. Thus, these results confirm that the docking method used is valid and reliable for evaluating ligand-receptor interactions in this study.

Based on the findings, natural flavonoid compounds such as quercetin, kaempferol, and apigenin found in the ethyl acetate fraction of *M pendens* exhibit strong interaction to MMP1. Figure 3 D-F shows selected potential compounds that demonstrate the best binding conformations with the receptors. The highest binding energies were quercetin for MMPs receptor with a binding energy of -9.6 kcal/mol, cholesta-22,24-dien-5-ol, 4,4-dimethyl-(22E)-4,4-dimethylcholesta-22,24-dien-6-ol for EGFR receptor with a binding energy of -9.1 kcal/mol, and procyanidin B1 for FGFRs receptor with a binding energy of -9.3 kcal/mol. Figure 3D illustrates the molecular interactions of compounds from the ethyl acetate fraction of *M. pendens* with the MMP receptor, showing several important molecular mechanisms. Hydrophobic interactions between the aromatic group of quercetin and hydrophobic residues such as Leu218

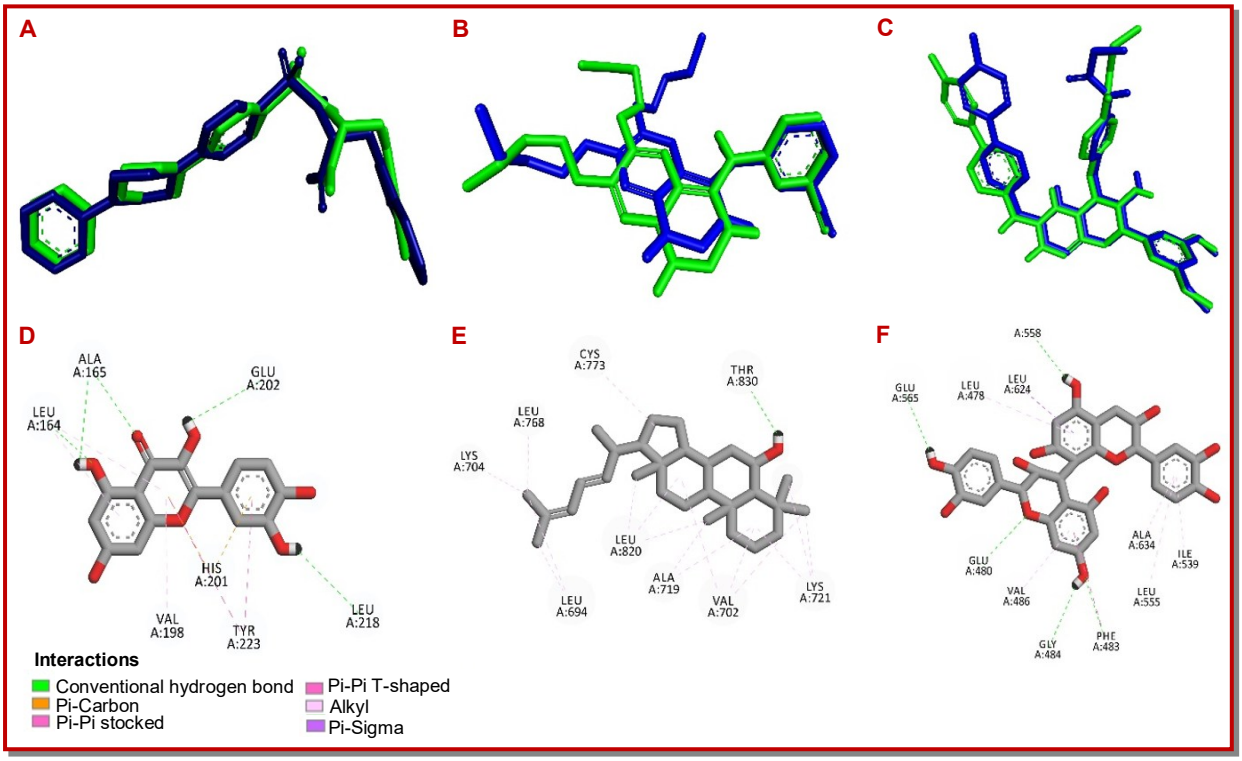

Figure 3: Native ligand (green) and native ligand redocked (blue) comparisons of MMP (A), EGFR (B), and FGFR (C). Binding of quercetin in the active site of MMP (D), binding of cholesta-22,24-dien-5-ol, 4,4-dimethyl-(22E)-4,4-dimethylcholesta-22,24-dien-6-ol in the active site of EGFR (E), binding of procyanidin B1 in the active site of FGFRs (F)

and Leu164 strengthen the binding of the compound to the active site.

Figure 3E shows the interaction of cholesta-22,24-dien-5-ol, 4,4-dimethyl-(22E)-4,4-dimethylcholesta-22,24-dien-6-ol from the ethyl acetate fraction of *M. pendens* with the EGFR receptor. The alkyl chain from the steroid compound interacts with hydrophobic residues such as Leu768, Leu694, Leu820, and Val702 through hydrophobic interactions. Figure 3F shows the interaction of procyanidin B1 from the ethyl acetate fraction of *M. pendens* with FGFRs, involving the formation of hydrogen bonds with residues such as Ala558, Glu565, Glu480, Gly484, and Phe483. This FGF interacted with the external domain of the receptor, which consists of subunits containing important residues like Glu565 and Glu480.

Diabetic wound healing

The morphological observation of wound healing at various time points for 14 days revealed significant differences between the negative control, positive control, and treatment groups with hydrogel based on the ethyl acetate fraction of *M pendens* (Figure 4). In the negative control group, wound healing was the slowest, with wound closure not reaching 50% by day 14. In the treatment group with 0.05% ethyl acetate hydrogel, wound contraction started to be visible by day 14, although scabbing was uneven and the wound was not fully healed, yet still better than the negative control. In the 0.10% concentration group, the wound was still relatively large on day 3, with a small amount of new tissue at the wound edges. By days 5 to 7, scabbing began to form, and by day 9, the wound showed shrinkage with slower epithelialization compared to the 0.15% concentration group. By day 14, the wound was only partially closed, with more noticeable scarring. In contrast, at the 0.15% concentration, the wound area began to shrink by day 3 with more uniform and rapid new tissue formation. Scabbing formed more quickly by days 5 to 7, and the wound shrank more significantly compared to the 0.05% concentration. By day 9, the wound was almost completely closed, and by day 14, the wound was fully closed with minimal scarring, indicating fast healing and effective remodeling. Hair growth was observed on the newly formed skin in the 0.15% fraction group, showing good skin function recovery.

Data analysis in Figure 4C showed that the negative control group experienced suboptimal wound healing, with a low percentage of wound closure (around 30-40%) by day 14. Meanwhile, the positive control (tetrachlorodecaoxide) showed significant improvement ($p<0.01$) from day 5, with wound closure reaching 80% by day 14. Hydrogel with 0.05% ethyl acetate fraction of *M. pendens* showed significant improvement compared to the negative control ($p<0.05$), although still slower than the higher concentrations, with 85% wound closure by day 14. The 0.10% concentration showed the best results, with the fastest and most significant wound closure at all time points ($p<0.001$), reaching 100% closure by day 14, compared to the positive control and other groups. Although the 0.15% concentration was effective, its speed was slightly slower compared to the 0.10%, with significant differences observed from days 7 to 14 ($p<0.05$).

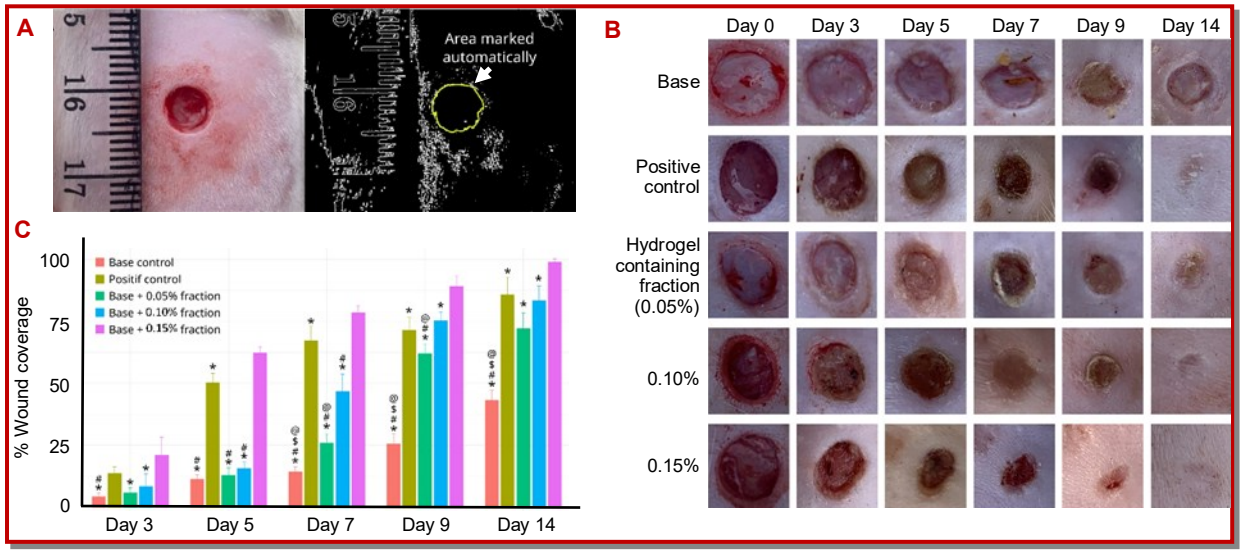

Figure 4: A) Picture of real wound with diameter by scale (left) and automatic wound marking (right, arrow head) by ImageJ software. B) Morphology of wound healing in diabetic rats following treatment with hydrogel based on the ethyl acetate fraction of *M pendens* at differences concentrations (0.05%, 0.10%, and 0.15%), compared to negative and positive controls. C) Wound closure of rats observed during the treatment. Note: (*, $p<0.05$) indicates a significant difference compared to the 0.15% group. (#, $p<0.05$) indicates a significant difference compared to the positive control group. (@, $p<0.05$) indicates a significant difference compared to the 0.10% group. ($, $p<0.05$) indicates a significant difference compared to the 0.05% group

Discussion

The phytochemical profile of *M. pendens* confirms the presence of several key secondary metabolites, including alkaloids, flavonoids, terpenoids, tannins, and saponins. The high concentration of flavonoids in the ethyl acetate fraction, recorded at 91.5 ± 0.0% QE, indicates that this fraction is particularly bioactive. This value is notably higher than that reported in a study, where documented 63.3 ± 1.8 mg QE/g in ethanolic extracts containing compounds like kaempferol, quercetin, and apigenin (Engida et al., 2015). Similarly, lower levels of rosmarinic acid and procyanidin B1 were observed in the ethyl acetate fraction, and even less in supercritical extracts (Larit et al., 2019).

FTIR analysis findings show that compounds such as rosmarinic acid, procyanidin B1, gallic acid, caffeic acid, ferulic acid, p-coumaric acid, quercetin, rutin, kaempferol, luteolin, apigenin, palmitic acid, oleic acid, cholesta-22,24-dien-5-ol, and 4,4-dimethyl are likely responsible for the observed peaks (Kanimozhi and Prasad, 2015).

On the other hand, the peak at 1393 cm^{-1} is a distinctive feature indicating the presence of compounds with an amide group (Lv et al., 2018; Ellerbrock and Gerke, 2021). Flavonoid compounds with an amide group identified in *M. pendens* include cinnamic acid and methanamide, which have shown anti-neurodegenerative effects (Hofmann et al., 2022), as well as strong anti-inflammatory, antibacterial, and antifungal properties (Wibawa et al., 2020; Chan et al., 2021).

Increased extract concentration was also associated with changes in physical characteristics of the formulation, such as stronger aroma and deeper color intensity. These sensory changes are likely due to the higher levels of terpenoids and phenolic compounds, which are known to produce distinctive scents and visual pigmentation (Gutierrez-del-Rio et al., 2021; Masyita et al., 2022). Flavonoids, in particular, contribute yellow hues, while tannins impart brown tones (Manzoor et al., 2021; Mallick et al., 2024). Both compound groups increase in concentration as the extract content rises, affecting the final appearance of the formulation. The observed increase in viscosity with higher extract concentrations is consistent with reports that flavonoids and tannins can interact with hydrogel matrices, such as hydroxypropyl methylcellulose, enhancing gel strength and formulation stability (Micale et al., 2020; Ferreira et al., 2024; Studzińska-Sroka et al., 2024; Valero et al., 2024). This not only improves texture but also helps retain the active ingredients longer on the skin, potentially enhancing therapeutic effect (Juncan et al., 2021; Salvioni et al., 2021; Studzińska-Sroka et al., 2024)

Molecular docking studies provide mechanistic insight into how the ethyl acetate fraction supports wound healing. Quercetin, a dominant flavonoid in the extract, interacts with MMPs by forming hydrogen bonds with key residues (e.g., Glu202 and His201), inhibiting enzymatic activity at the catalytic site (Liu et al., 2021; Li et al., 2024). Inhibition of MMP-1, -2, and -9 reduces ECM degradation, a process that is often excessive in diabetic wounds and contributes to poor healing (Varghese et al., 2021; Liang et al., 2023). Quercetin also disrupts signaling pathways such as NF-κB and MAPK, downregulating MMP gene expression. Moreover, it promotes the expression of TIMPs (tissue inhibitors of metalloproteinases), helping restore protease balance and supporting ECM stabilization (Fu et al., 2022; Kamal et al., 2024). Hydrogen bonds occur between the hydroxyl group of the steroid compound and amino acid residues such as Thr830, which contains a hydroxyl group on its side chain, and alkyl interactions with amino acid residues like Leu768, Lys704, Cys773, Leu694, Leu820, Ala719, Val702, and Lys721 at the active site of EGFR, which play a key role in modulating EGFR activation and related signaling pathways (Panigrahi, 2008).

Other compounds, including steroid derivatives like cholesta-22,24-dien-5-ol, demonstrate interaction with EGFR through hydrogen bonding with key residues such as Leu768 and Lys721. These interactions facilitate conformational changes necessary for EGFR activation and subsequent signaling through the MAPK and PI3K/Akt pathways. This activation promotes keratinocyte proliferation and migration, which are critical for wound closure (Xu et al., 2023). Additionally, interactions with FGFR via compounds like procyanidin B1 suggest activation of angiogenic pathways. Binding with residues such as Lys704 and His553 initiates receptor dimerization and tyrosine phosphorylation, triggering downstream signaling cascades involved in fibroblast migration and neovascularization. The presence of glycosaminoglycan-binding residues also enhances FGFR activation, contributing to tissue regeneration (Shanmugam et al., 2022).

The *in vivo* results suggest that the wound healing efficacy of the ethyl acetate fraction of *M. pendens* is positively correlated with concentration. The gradual enhancement of healing with increasing doses indicates that the bioactive constituents actively promote key regenerative processes, such as fibroblast proliferation, extracellular matrix remodeling, and neovascularization (Addis et al., 2020). Although minor variations in healing speed were observed between concentrations, the highest concentration (0.15%) ultimately achieved the most complete wound closure, implying that higher doses maintain sufficient biological activity to overcome potential delays in the early phases of repair. This trend supports the notion that, within the tested range, increasing concentration does not induce cytotoxic effects severe enough to impair healing. Instead, the data emphasizes the potential for dose escalation to

achieve maximal therapeutic outcomes, highlighting the importance of careful dose optimization when developing phytochemical-based wound healing therapies.

Beyond enhancing wound closure rates, treatment with the ethyl acetate fraction markedly improved the quality of wound remodeling. The absence of scab formation throughout the healing process, coupled with the lack of visible scar tissue, suggests that the extract modulated the repair process toward a regenerative rather than a fibrotic pathway (Mamun et al., 2024). This phenomenon may reflect a favorable influence on keratinocyte proliferation and migration, as well as modulation of myofibroblast activity, minimizing excessive extracellular matrix deposition (Dong et al., 2025). These *in vivo* outcomes are consistent with molecular docking findings, which showed that major bioactive compounds in the fraction, such as quercetin and steroid derivatives, interact with key targets like MMPs, EGFR, and FGFR to regulate ECM stability, promote keratinocyte activation, and stimulate angiogenesis. Moreover, the observed regrowth of hair follicles at the wound site indicates successful restoration of dermal architecture and adnexal structures, implying activation of resident stem cell populations and full reestablishment of skin function. Collectively, these findings position the ethyl acetate fraction of *M. pendens* as a promising candidate not only for accelerating wound closure but also for promoting functional tissue regeneration, a hallmark objective in the development of next-generation wound therapeutics.

This study was limited to *in silico*, *in vitro*, and short-term *in vivo* evaluations, which may not fully reflect the long-term safety and efficacy of *M. pendens* hydrogel in clinical settings. The *in vivo* tests were conducted on a rat animal model, and the findings may not be directly applicable to human physiology. Furthermore, the investigation focused solely on selected molecular pathways (MMP, EGFR, FGFR), while other important mechanisms involved in diabetic wound healing such as inflammatory cytokines and angiogenesis factors were not assessed.

Conclusion

The ethyl acetate fraction of *M. pendens* demonstrates therapeutic potential for diabetic wound healing by inhibiting MMPs and activating EGFR and FGFR pathways. Its rich phytochemical content and *in vivo* efficacy support further development into advanced pharmaceutical formulations.

Financial Support

This research is funded through the Hibah Penelitian Dosen Pemula Kemendikbud (Ministry of Education and Culture) No. 106/E5/PG.02.00.PL/2024.

Ethical Issue

The preparation process and animal wound healing tests were approved by the Ethics Committee (KEPK), Faculty of Pharmacy, Universitas Muhammadiyah Ahmad Dahlan Cirebon, under approval number 003/VIII/2024/9110/KEPK/STFMC. Animal handling in this study followed the AECD guidelines.

Conflict of Interest

Authors declare no conflict of interest

Acknowledgement

The first author would like to thank the Pharmacognosy and Natural Products Laboratory, as well as the Pharmacology Laboratory, Faculty of Pharmacy, Universitas Islam Kalimantan Muhammad Arsyad Al Banjari, for their support and the facilities provided. We would also like to thank Dr. Renny Amelia, for the help in statistical analysis.

References

Addis R, Cruciani S, Santaniello. Fibroblast proliferation and migration in wound healing by phytochemicals: Evidence for a novel synergic outcome. Int J Med Sci. 2020; 17: 1030-42.

Adeleke O, Oboh G, Adefegha S, Osesusi A. Effect of aqueous extract from root and leaf *of Sphenocentrum jollyanum* Pierre on wounds of diabetic rats: Influence on wound tissue cytokines, vascular endothelial growth factor and microbes. J Ethnopharmacol. 2022; 293: 115266.

Alexiadou K, Doupis J. Management of diabetic foot ulcers. Diabetes Ther. 2012; 3: 3-4.

Baskakov OI, Horneman VM, Lohilahti J, Alanko S. High resolution FTIR spectra of the ν9 vibrational band of cis-rotamers HCOOH and H13COOH. J Mol Struct. 2006; 795: 49-53.

Boulton AJM, Whitehouse RW. The diabetic foot. 2000.

Burgess JL, Wyant WA, Abdo Abujamra B, Kirsner RS, Jozic I. Diabetic wound-healing science. Medicina (B Aires) 2021; 57: 1072.

Chan CF, Liu Z, Wong. Amine-linked flavonoids as agents against cutaneous leishmaniasis. Antimicrob Agents Chemother. 2021; 65.

Chanu NR, Gogoi P, Barbhuiya PA, Dutta PP, Pathak MP, Sen S. Natural flavonoids as potential therapeutics in the management of diabetic wound: A review. Curr Top Med Chem. 2023; 23: 690-710.

Cheng YZ, Liu IM, Cheng JT, Lin BS, Liu F. Wound healing is promoted by *Musa paradisiaca* (banana) extract in diabetic rats. Arch Med Sci. 2020.

Chu LK, Huang YH, Lee YP. Step-scan FTIR techniques for investigations of spectra and dynamics of transient species in gaseous chemical reactions. Molecular and laser spectroscopy. New York, Elsevier, 2022, pp 481-527.

Dasari N, Jiang A, Skochdopole A, Chung J, Reece EM, Vorstenbosch J, Winocour S. Updates in diabetic wound healing, inflammation, and scarring. Semin Plast Surg. 2021; 35: 153-58.

Daulay M, Syahputra M, Sari M, Widyawati T, Anggraini D. The potential of *Myrmecodia pendans* in preventing complications of diabetes mellitus as an antidiabetic and antihyperlipidemic agent. Open Vet J. 2024; 14: 1607.

Dirgantara S, Insanu M, Fidrianny I. Medicinal properties of ant nest plant (*Myrmecodia* Genus): A comprehensive review. Open Access Maced J Med Sci. 2022; 10: 97-103.

Dong X, Xiang H, Li Jiajia, Hao. Dermal fibroblast-derived extracellular matrix (ECM) synergizes with keratinocytes in promoting re-epithelization and scarless healing of skin wounds: Towards optimized skin tissue engineering. Bioact Mater. 2025; 47: 1-17.

Ellerbrock RH, Gerke HH. FTIR spectral band shifts explained by OM–cation interactions. J Plant Nutr Soil Sci. 2021; 184: 388-97.

Engida AM, Faika S, Nguyen-Thi BT, Ju Y-H. Analysis of major antioxidants from extracts of *Myrmecodia pendans* by UV/visible spectrophotometer, liquid chromatography/tandem mass spectrometry, and high-performance liquid chromatography/UV techniques. J Food Drug Anal. 2015; 23: 303-09.

Ferreira LM de MC, Modesto YY, Souza. Characterization, biocompatibility and antioxidant activity of hydrogels containing propolis extract as an alternative treatment in wound healing. Pharmaceuticals 2024; 17: 575.

Fu K, Zheng X, Chen Y, Wu L, Yang Z, Chen X, Song W. Role of matrix metalloproteinases in diabetic foot ulcers: Potential therapeutic targets. Front Pharmacol. 2022; 2022.

Gartika M, Pramesti HT, Kurnia D, Satari MH. A terpenoid isolated from sarang semut (*Myrmecodia pendans*) bulb and its potential for the inhibition and eradication of *Streptococcus mutans* biofilm. BMC Complement Altern Med. 2018; 18: 151.

Gutierrez-del-Río I, Lopez-Ibanez S, Magadan-Corpas P, Fernandez-Calleja L, Perez-Valero A, Tunon-Granda M, Miguelez EM, Villar CJ, Lombo F. Terpenoids and polyphenols as natural antioxidant agents in food preservation. Antioxidants 2021; 10: 1264.

Hofmann J, Spatz P, Walther R, Gutmann M, Maurice T, Decker M. Synthesis and biological evaluation of flavonoid-cinnamic acid amide hybrids with distinct activity against neurodegeneration *in vitro* and *in vivo*. Chem A Eur J. 2022; 28.

Juncan AM, Moisa DG, Santini A, Morgovan C, Rus LL, Vonica-Ţincu AL, Loghin F. Advantages of hyaluronic acid and its combination with other bioactive ingredients in cosmeceuticals. Molecules 2021; 26: 4429.

Kamal R, Awasthi A, Pundir M, Thakur S. Healing the diabetic wound: Unlocking the secrets of genes and pathways. Eur J Pharmacol. 2024; 975: 176645.

Kanimozhi G, Prasad NR. Anticancer effect of caffeic acid on human cervical cancer cells. Coffee in health and disease prevention. New York, Elsevier, 2015, pp 655-61.

Kementerian Kesehatan RI. Farmakope herbal Indonesia. II. Jakarta, Kementerian Kesehatan RI, 2017.

Kuswandani F, Satari MH, Maskoen AM. Antimicrobial efficacy of *Myrmecodia pendens* extract and fraction combination against enter action combination against *Enterococcus faecalis* ATCC 29212. J Dent Indones. 2019; 26: 119-25.

Larit F, Leon F, Benyahia S, Cutler SJ. Total phenolic and flavonoid content and biological activities of extracts and isolated compounds of *Cytisus villosus* Pourr. Biomolecules 2019; 2019.

Li K, Wang Y, Liu W, Zhang C, Xi Y, Zhou Y, Li H, Liu X. Structure–activity relationships and changes in the inhibition of xanthine oxidase by polyphenols: A review. Foods 2024; 13: 2365.

Liang D, Liu L, Zhao Y, Luo Z, He Y, Li Y, Tang S, Tang J and Chen N. Targeting extracellular matrix through phytochemicals: A promising approach of multi-step actions on the treatment and prevention of cancer. Front Pharmacol. 2023; 2023.

Lisnanti EF, Lokapirnasari WP, Hestianah EP, Al Arif MA, Baihaqi ZA, Yulianto AB. Antibacterial alternatives using the potential of the ant nest plant (Myrmecodia spp.). Int J One Health. 2024; 10: 148-52.

Liu Y, Liu Y, Deng J, Li W, Nie X. Fibroblast growth factor in diabetic foot ulcer: Progress and therapeutic prospects. Front Endocrinol (Lausanne). 2021; 12: 744868.

Lv BH, Tan W, Zhu CC, Shang X, Zhang L. Properties of a stable and sustained-release formulation of recombinant human parathyroid hormone (rhPTH) with chitosan and silk fibroin microparticles. Med Sci Monit. 2018; 24: 7532-40.

Mallick SR, Hassan J, Hoque MdA, Sultana H, Kayesh E, Ahmed. Color, proximate composition, bioactive compounds and antinutrient profiling of rose. Sci Rep. 2024; 14: 21690.

Mamun A Al, Shao C, Geng P, Wang S, Xiao J. Recent advances in molecular mechanisms of skin wound healing and its treatments. Front Immunol. 2024; 2024.

Manzoor M, Singh J, Gani A, Noor N. Valorization of natural colors as health-promoting bioactive compounds: Phytochemical profile, extraction techniques, and pharmacological perspectives. Food Chem. 2021; 362: 130141.

Masyita A, Mustika Sari R, Dwi Astuti A, Yasir. Terpenes and terpenoids as main bioactive compounds of essential oils, their roles in human health and potential application as natural food preservatives. Food Chem X. 2022; 13: 100217.

McDermott K, Fang M, Boulton AJM, Selvin E, Hicks CW. Etiology, epidemiology, and disparities in the burden of diabetic foot ulcers. Diabetes Care. 2023; 46: 209-21.

Micale N, Citarella A, Molonia MS, Speciale A, Cimino F, Saija A, Cristani M. Hydrogels for the delivery of plant-derived (poly)phenols. Molecules 2020; 25: 3254.

Najah, A. S., Kilo, A. La, Kadir, A. Potential effects of *Myrme-*

codia pendans (ant nests) on healing bone injuries. 2024; 13: 311-19.

Ol'ha OB, Hovorun DM. Conformational equilibrium, IR and Raman vibrational spectra of the quercetin molecule in different solvents: A comprehensive quantum-chemical investigation. Chem Phys Impact. 2021; 3: 100033.

Panigrahi SK. Strong and weak hydrogen bonds in protein-ligand complexes of kinases: A comparative study. Amino Acids. 2008; 34: 617-33.

Primasari A, Apriyanti E, Ambardhani N, Satari MH, Herdiyati Y, Kurnia D. Formulation and antibacterial potential of sarang semut (*Myrmecodia pendans*) against oral pathogenic bacteria: An *in vitro* study. Open Dent J. 2022; 2022.

Salvioni L, Morelli L, Ochoa E, Labra. The emerging role of nanotechnology in skincare. Adv Colloid Interface Sci. 2021; 293: 102437.

Shanmugam L, Anuja AV, Rajinikanth SK, Samuel PJ. Epidermal growth factor (EGF) in wound repair. Therapeutic proteins against human diseases. Singapore, Springer Nature, 2022, pp 29-49.

Soheilifar MH, Dastan D, Masoudi-Khoram N, Keshmiri Neghab H, Nobari S, Tabaie SM, Amini R. *In vitro* and *in vivo* evaluation of the diabetic wound healing properties of saffron (*Crocus sativus* L.) petals. Sci Rep. 2024; 14: 19373.

Spampinato SF, Caruso GI, De Pasquale R, Sortino MA, Merlo S. The treatment of impaired wound healing in diabetes: Looking among old drugs. Pharmaceuticals 2020; 13: 60.

Studzinska-Sroka E, Paczkowska-Walendowska M, Erdem. Anti-aging properties of chitosan-based hydrogels rich in bilberry fruit extract. Antioxidants 2024; 13: 105.

Sudiono J, Oka C, Trisfilha P. The scientific base of *Myrmecodia pendans* as herbal remedies. Br J Med Med Res. 2015; 8: 230-37.

Sulastri E, Zubair MS, Anas NI, Abidin S, Hardani R, Yulianti R. Total phenolic, total flavonoid, quercetin content and antioxidant activity of standardized extract of *Moringa oleifera* leaf from regions with different elevation. Pharmacogn J. 2018; 10: s104-08.

Valero L, Gainche M, Esparcieux C, Delor-Jestin F, Askanian H. Vegetal polyphenol extracts as antioxidants for the stabilization of PLA: Toward fully biobased polymer formulation. ACS Omega. 2024; 2024.

Varghese A, Chaturvedi SS, Fields GB, Karabencheva-Christova TG. A synergy between the catalytic and structural Zn (II) ions and the enzyme and substrate dynamics underlies the structure-function relationships of matrix metalloproteinase collagenolysis. J Biol Inorg Chem. 2021; 26: 583-97.

Vinodh R, Sangeetha D. Quaternized poly(styrene ethylene butylene poly styrene)/multiwalled carbon nanotube composites for alkaline fuel cell applications. J Nanosci Nanotechnol 2013;13:5522–33.

Wibawa IPAH, Andila PS, Saraswaty V, Tirta IG. Phytochemical properties and antioxidant activities of the leaf extracts of *Boenninghausenia albiflora* (Hook.) Rchb. ex. Meisn. (Rutaceae). Berkala Penelitian Hayati. 2020; 25: 12-17.

Widyawati T, Pase MA, Daulay M, Sumantri IB, Yusoff NA. Evaluation of *Myrmecodia pendans* water extracts on hematology profiles, liver, kidney function and malondialdehyde level in healthy volunteer. Pharmacogn J. 2020; 12: 1489-93.

Xu Y, Hu Q, Wei Z, Ou. Advanced polymer hydrogels that promote diabetic ulcer healing: Mechanisms, classifications, and medical applications. Biomater Res. 2023; 2023.

Author Info

Abd Kakhar Umar (Principal contact)
e-mail: abd.kakhar@etflin.com